



Equilibration dynamics in heavy-ion reactions

Yoritaka Iwata (GSI, Darmstadt)



ExtreMe Matter Institute EMMI



Contents

- Dynamics via **nucleus-nucleus potential [1]**
- Dynamics at the early stage
 - dynamics governed by **charge equilibration [2]**
 - dissipation in TD-DFT [2,3]**

[1] Y.I., EPJW (CNR* 11), to appear

[2] Y.I.-Otsuka-Maruhn-Itagaki, PRL(2010);
Y.I.-Otsuka-Maruhn-Itagaki, NPA(2010);
Y.I.-Otsuka-Maruhn-Itagaki, EPJA(2009);
Y.I. Scitopics, Elsevier (2010);

[3] Y.I.-Maruhn, PRC (2011)

TD-DFT (TDHF)

Discuss reaction mechanism
based on microscopic time-dependent density functional calculations

Skryme Energy density functional (Skryme EDF)

q = p, n

(i) particle density,

$$\rho(\mathbf{r}) = \rho(\mathbf{r}, \mathbf{r}),$$

(ii) kinetic energy density,

$$\tau(\mathbf{r}) = [\nabla \cdot \nabla' \rho(\mathbf{r}, \mathbf{r}')]_{\mathbf{r}=\mathbf{r}'},$$

(iii) spin density,

$$s(\mathbf{r}) = s(\mathbf{r}, \mathbf{r}),$$

(iv) momentum density,

$$\mathbf{j}(\mathbf{r}) = \frac{1}{2i} [(\nabla - \nabla') \rho(\mathbf{r}, \mathbf{r}')]_{\mathbf{r}=\mathbf{r}'},$$

(v) spin current tensor,

$$J_{\mu\nu}(\mathbf{r}) = \frac{1}{2i} [(\nabla_\mu - \nabla'_\mu) s_\nu(\mathbf{r}, \mathbf{r}')]_{\mathbf{r}=\mathbf{r}'},$$

(vi) kinetic energy density (vector part)

$$\mathbf{T}(\mathbf{r}) = [\nabla \cdot \nabla' s(\mathbf{r}, \mathbf{r}')]_{\mathbf{r}=\mathbf{r}'},$$

Master eq. (variational principle)

$$\delta E = \sum_q \int d^3r \left\{ \frac{\hbar^2}{2m_q^*} \delta\tau_q(\mathbf{r}) + U_q(\mathbf{r}) \delta\rho_q(\mathbf{r}) + \vec{B}_q(\mathbf{r}) \cdot \vec{\delta J}_q(\mathbf{r}) + \mathbf{I}_q(\mathbf{r}) \cdot \delta\mathbf{j}_q(\mathbf{r}) \right. \\ \left. + \mathbf{C}_q(\mathbf{r}) \cdot \delta\mathbf{T}_q(\mathbf{r}) + \Sigma_q(\mathbf{r}) \delta s_q(\mathbf{r}) \right\} = 0$$

where

$$\frac{\hbar^2}{2m_q^*} = \frac{\hbar^2}{2m} + \frac{1}{4}(t_1 + t_2)\rho + \frac{1}{8}(t_2 - t_1)\rho_q,$$

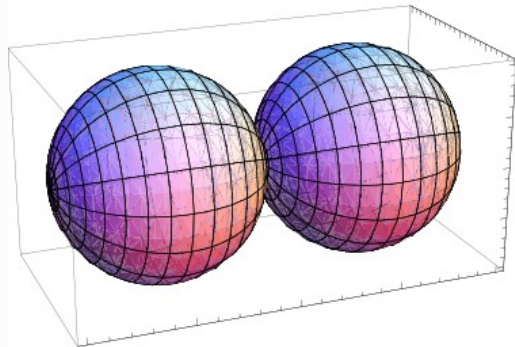
$$U_q(\mathbf{r}) = t_0[(1 + \frac{1}{2}x_0)\rho - (x_0 + \frac{1}{2})\rho_q] + \frac{1}{8}(t_2 - 3t_1)\nabla^2\rho + \frac{1}{16}(3t_1 + t_2)\nabla^2\rho_q \\ + \frac{1}{4}(t_1 + t_2)\tau + \frac{1}{8}(t_2 - t_1)\tau_q + \frac{1}{4}t_3(\rho^2 - \rho_q^2 - (s - s_q)^2) - \frac{1}{2}V_{s.o.} \vec{\nabla} \cdot (\vec{J} + \vec{J}_q),$$

$$\vec{B}_q = -\frac{1}{4}(t_2 - t_1)\vec{J}_q + \frac{1}{2}V_{s.o.} \vec{\nabla}(\rho + \rho_q),$$

$$\mathbf{I}_q(\mathbf{r}) = -\frac{1}{2}(t_1 + t_2)\mathbf{j} - \frac{1}{4}(t_2 - t_1)\mathbf{j}_q - \frac{1}{2}V_{s.o.} \nabla \times (s + s_q),$$

$$\mathbf{C}_q(\mathbf{r}) = \frac{1}{8}(t_2 - t_1)\mathbf{s}_q,$$

$$\Sigma_q(\mathbf{r}) = \frac{1}{2}t_0(x_0 s - s_q) + \frac{1}{8}(t_2 - t_1)\mathbf{T}_q + \frac{1}{16}(t_2 + 3t_1)\nabla^2 s_q - \frac{1}{2}t_3(\rho - \rho_q)\mathbf{s}_q - \frac{1}{2}V_{s.o.} \nabla \times (\mathbf{j} + \mathbf{j}_q).$$



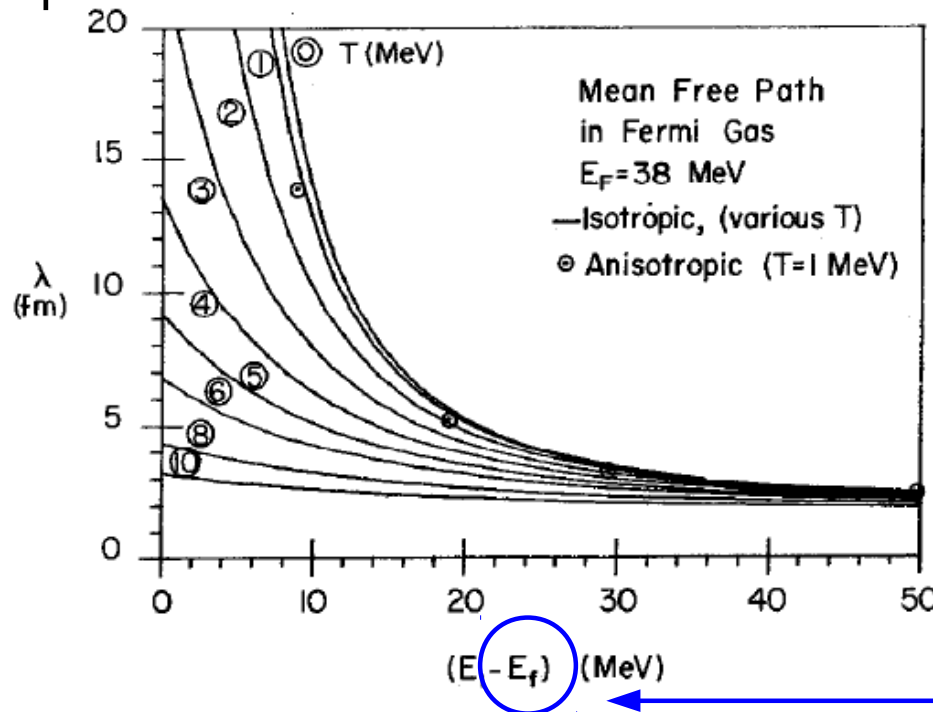
$$i\hbar \frac{\partial}{\partial t} \phi_j(\mathbf{r}, t) = H \phi_j(\mathbf{r}, t), \quad j = 1, \dots, A$$

Engel *et. al*, NPA (1975)

- Nice description in low-energy HIC

“(roughly) the radius of a nucleus < 10 fm ($R = 1.2 * A^{(1/3)}$)”
Collision times for a nucleon passing through 20 fm is the problem:

Mean free path of a nucleus



Let us assume the situation with colliding ground state nuclei with boost:

If the energy is set to the Fermi energy (25 ~ 30% of the speed of light) + 10 MeV/A, the mean-free path is less than 20 fm.

If the incident energy is less than that, the expected collision time becomes less than 1.

→ Collisionless framework such as TDDFT is sufficient to study low-energy heavy-ion collision

Fig. 2. The calculated nucleon mean free path, λ , in a nuclear Fermi gas of temperature T and Fermi energy, $E_F = 38$ MeV. The nucleon mean free path is given as a function of its energy above the Fermi energy, $(E_1 - E_F)$, for various values of T . The curves are obtained by calculating the expression (9), which assumes isotropic differential cross sections. The four circled points are computed from (8) using more realistic anisotropic cross sections and a temperature of $T = 1$. They show that the error involved in the isotropic assumption is not important in the present discussion.

- **“Diabatic”** Nucleus-Nucleus Potential from TD-DFT

More accurately, discuss reaction mechanism:
charge equilibration and dissipation due to LS-force

[Microscopic] TD-DFT (time-dependent density functional calculations; formerly known as TDHF, more terms are included, which is not classified to the mean-field, e.g. SKI sets)



“derive”

[Macroscopic] Collective Lagrangian

The potential structure, viscosity ...

Based on a traditional method

Koonin, Prog. Part. Nucl. Phys (1980)
Lacroix, arXiv:nucl-th/0202063.
Washiyama-Lacroix, PRC(2008).
Washiyama-Lacroix-Ayik, PRC (2009).

TDHF nucleus-nucleus Potential (collaboration with H. Feldmeier)

a few things to be noticed in advance

purely diabatic potential;

for adiabatic one, see Umar-Oberacker PRC (2006)

potential for excited states;

Potential for states far from the thermal equilibrium

vivid momentum dependence compared to adiabatic ones

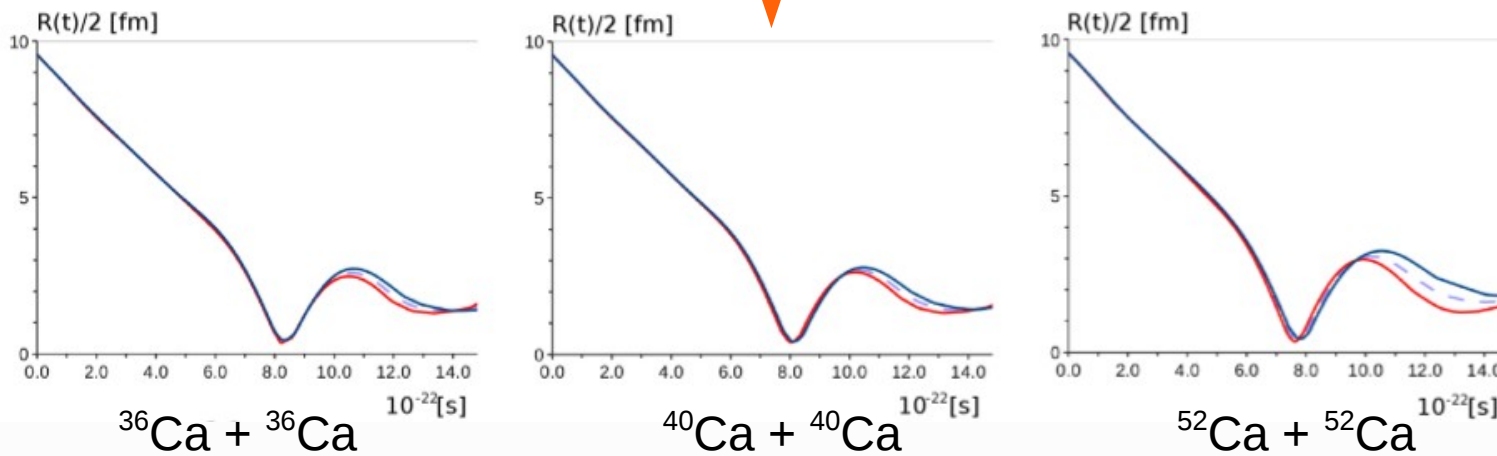
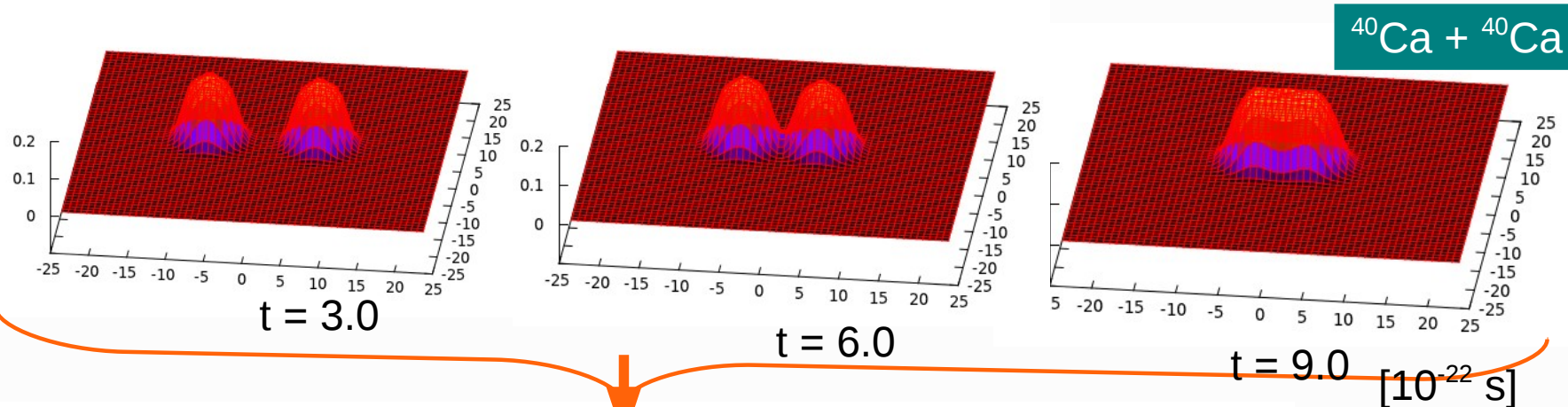
The introductory part of our method is shown.

- Recipe 1/2: Extract collective dynamics from microscopic calculation

Define collective variable using microscopically calculated results:

$$R(t) = 2 \int \int \int |z| \rho(t, x, y, z) dx dy dz$$

The definition of $R(t)$ is not unique



The relative velocity is fixed to 0.1c: low-energy heavy-ion collision

- Recipe 2/2: Find Collective Lagrangian -
 substitute $R(t)$ to macroscopic Lagrangian -

$$R(t) = 2 \int \int \int |z| \rho(t, x, y, z) dx dy dz$$

The definition of $R(t)$ is not unique

$$\frac{d}{dt} \frac{\partial \mathcal{L}}{\partial \dot{R}} - \frac{\partial \mathcal{L}}{\partial R} = Q; \quad \mathcal{L} = \frac{1}{2} \mu(R) \dot{R}^2 - V(R),$$

For example, it can be written by

$$\mu \ddot{R}(t) + \frac{1}{2} \frac{d\mu}{dR} \dot{R}(t)^2 + \frac{dV}{dR} + \gamma \dot{R}(t) = 0,$$

Effective mass
is R dependent

For example,
 Q term is assumed to be friction

- Checking method of non-zero viscosity (Q)
to appear in Y.I. EPJW (CNR*11)

We will show here the very introductory part of our research
For reference, we calculate the following two quantities:

$$(*) \quad \bar{\mu} \ddot{R}(t) + \frac{dV}{dR} = 0, \quad \text{Start with simplified situation}$$

$$\left\{ \begin{array}{l} V(R(t)) = E - \frac{1}{2} \bar{\mu} \dot{R}(t)^2 \end{array} \right. \quad (\text{eq. 1})$$

$$\left\{ \begin{array}{l} V(R(t)) - V(R_0) = -\bar{\mu} \int_{t_0}^t \ddot{R}(\tau) \dot{R}(\tau) d\tau \end{array} \right. \quad (\text{eq. 2})$$

Eliminating $V(R)$, we have

True if $R(t)$ satisfies Eq. (*)

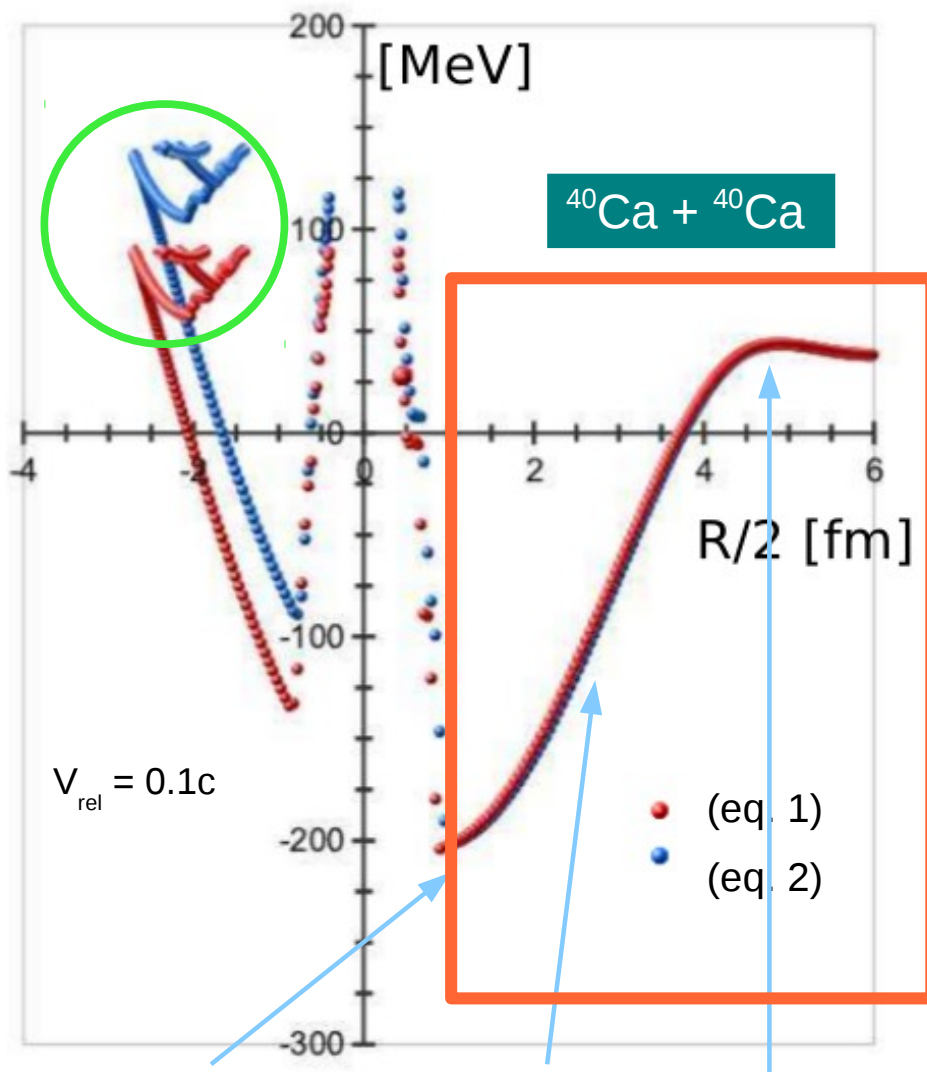
$$E = \frac{1}{2} \bar{\mu} \dot{R}(t)^2 + V(R_0) - \bar{\mu} \int_{t_0}^t \ddot{R}(\tau) \dot{R}(\tau) d\tau$$

Full expression of energy (to be compared)

$$\frac{1}{2} \mu(t) \dot{R}(t)^2 + V(R_0) - \int_{t_0}^t \mu(\tau) \ddot{R}(\tau) \dot{R}(\tau) d\tau + \delta E(t, \dot{R}),$$

• Calculated diabatic potential (TDHF potential)

Time evolutionary plot of the potential



Points to see :

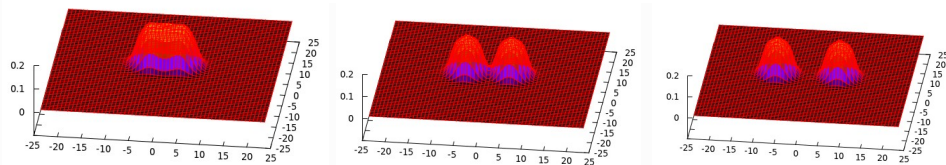
- ✓ The value (eq.1) means the loss of kinetic energy, and the value (eq.2) is obtained by assuming the potential form (for the interaction).

- ✓ If the values obtained by (eq.1) and (eq.2) is equal, then there is no viscosity.
→ there is no viscosity for the first approaching phase

- ✓ The positive side of R means time-evolution **before** the full-overlap, and its negative side shows the time-evolution **after** the full overlap.

- ✓ There is a rebound around $R/2 = -3$ [fm]; **marked by a green circle**. This is related to the effect of wall in the context of wall-window mechanism of dissipation.

- ✓ Curve in first approaching is regarded as the potential (**curve shown in the orange box**)



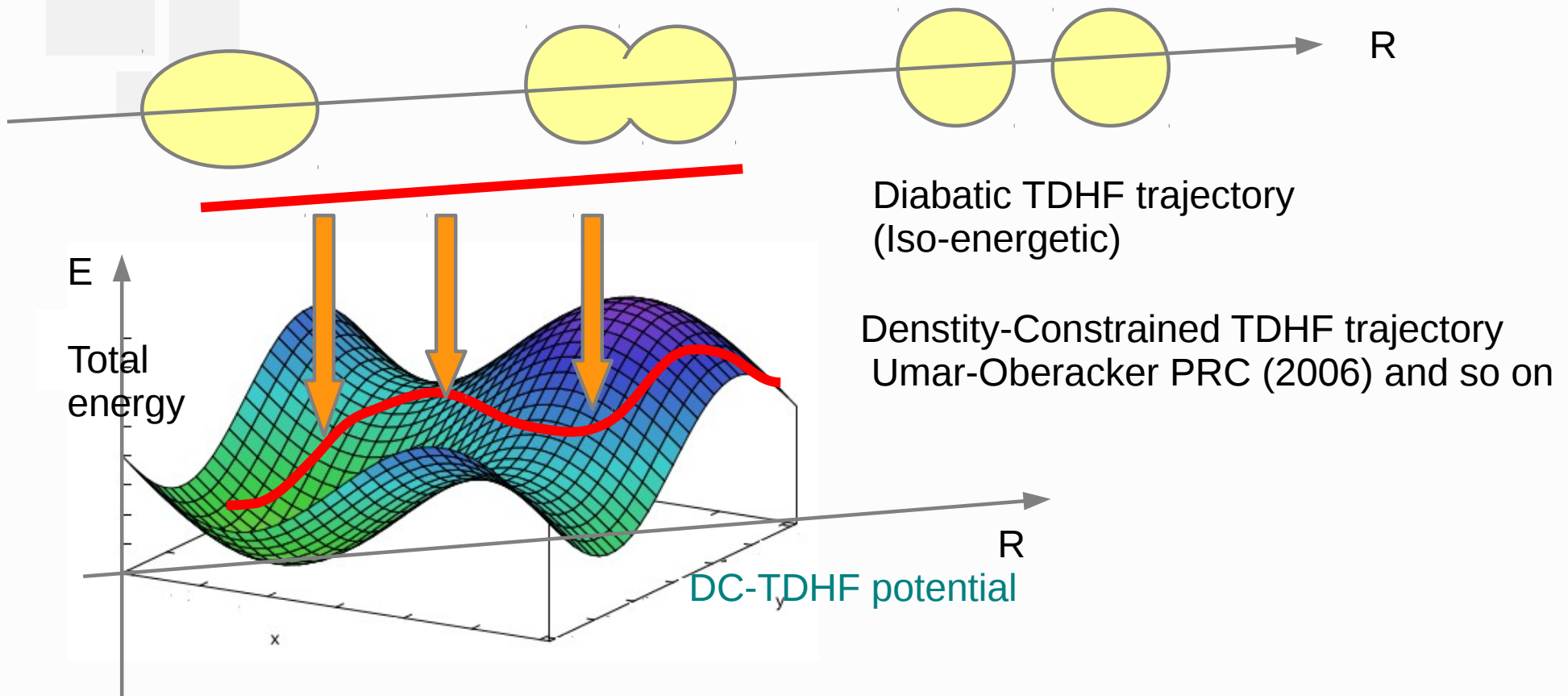
Time evolution is connected to R evolution

Radius of $^{40}\text{Ca} \sim 4.1$ fm

Coulomb barrier height of $^{40}\text{Ca} + ^{40}\text{Ca}$ ($R/2 = 4.1$) ~ 65 MeV

• Diabatic (far from the thermal equilibrium)

v.s. Adiabatic (almost the thermal equilibrium)



For adiabatic time evolution, the conservation of total energy is not necessarily true because of the additional cooling. However, for diabatic dynamics the total energy is strictly conserved.

Accordingly, potential obtained from our method and Density-constrained TDHF must not be the same; simply speaking, potentials are calculated for exactly different states.

[Reference results] TDHF results are confirmed to be far from the thermal equilibrium (Loebl-Maruhn-Reinhard, PRC (2010))

Charge equilibration

- an important mechanism in low-energy heavy-ion collisions -

(Fast) charge equilibration

_ prevents to produce exotic nuclei
decisive mechanism of exotic nuclear synthesis

_ very fast mechanism taking only $\sim 10^{-22}$ s

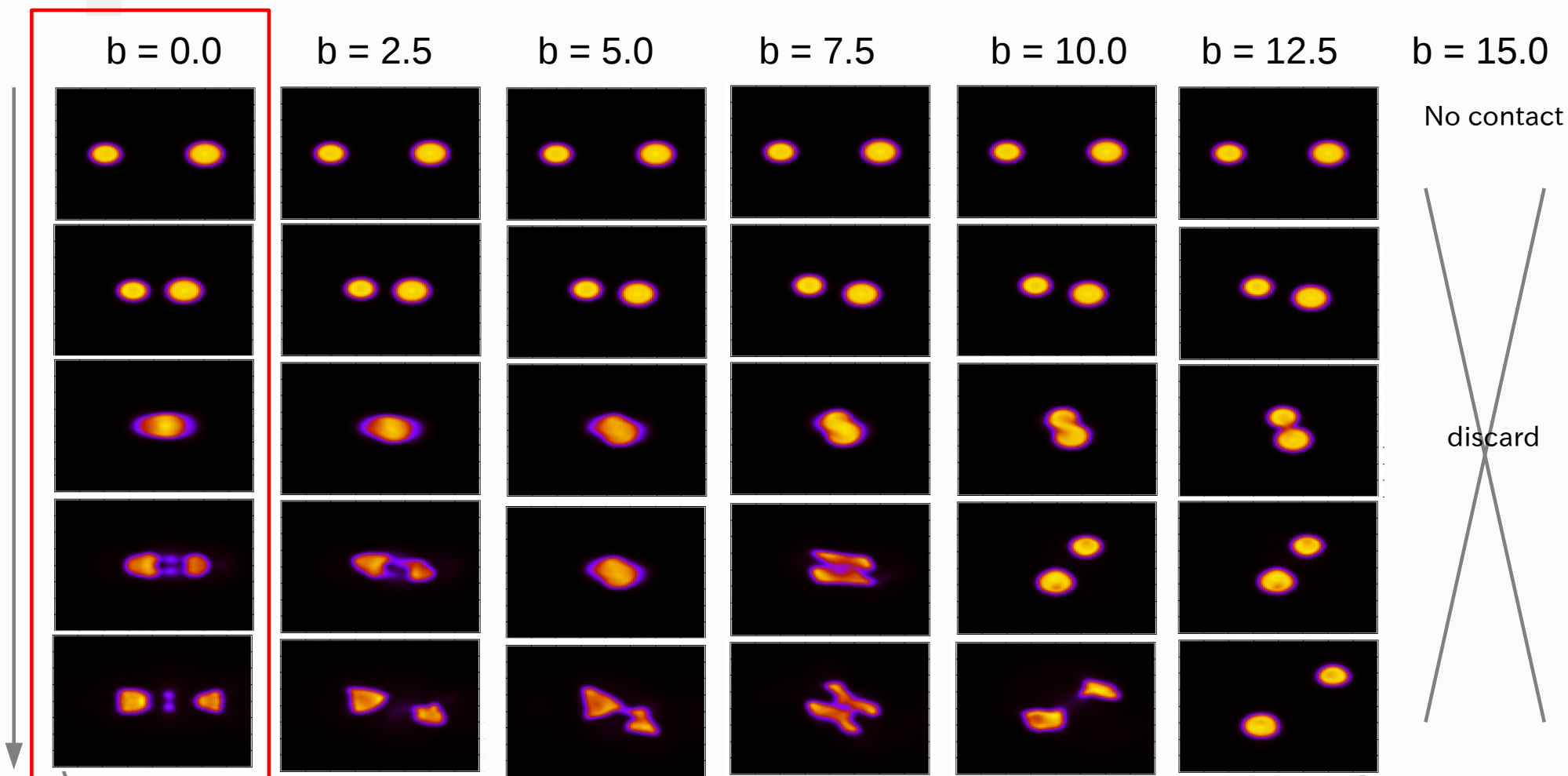
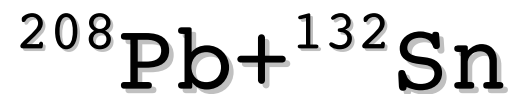
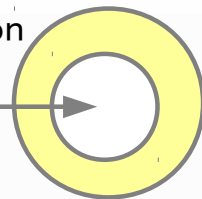
governing the early stage of heavy-ion collision

Y.I. et al., PRL (2010)

- There exists the upper-limit energy for the charge equilibration.
- The mechanism of (fast) charge equilibration is ultimately reduced to the nucleons with the Fermi velocity.

例) $E/A = 6.0 \text{ MeV}$

Reaction cross section
Is prop. to the area



time

head-on

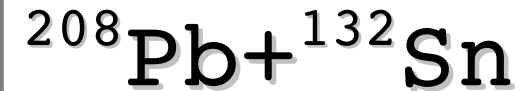
Superpose → compare to the experiment

notice) fragments are identified after sufficient time
no interference effect is included

- Distribution of final products based on 3d TD-DFT (SLy4)

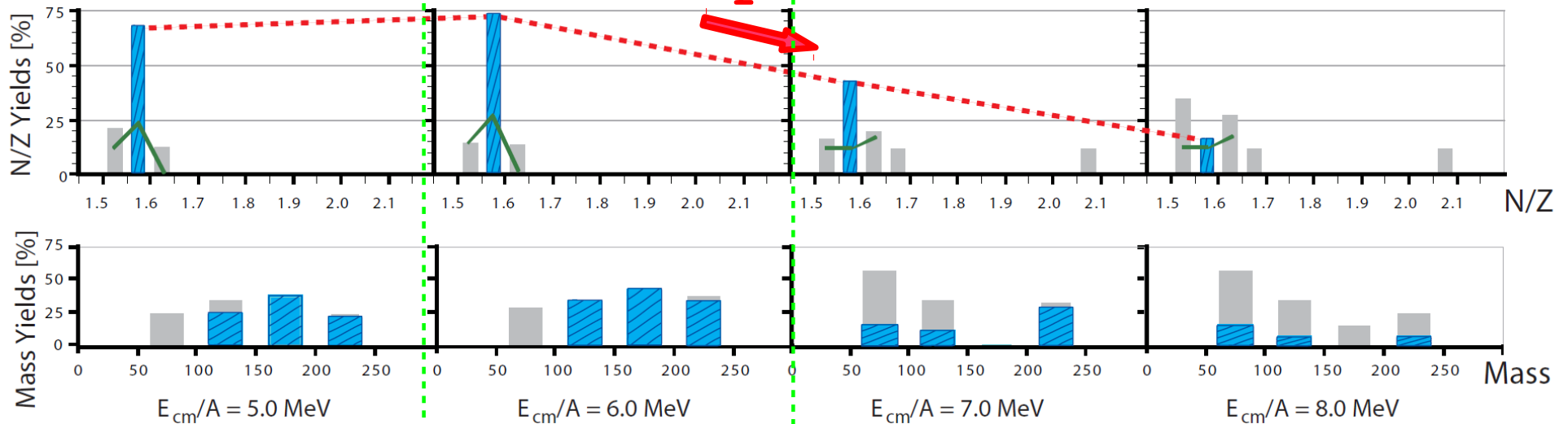
■ : charge equilibrated products

charge equilibrium: $208/132 = 1.58$



Flat

Sharp decrease



Charge is equilibrated
(rate: more than 50%)

Energy
Threshold
($6.5\text{MeV} \pm 0.5\text{MeV}$)

Charge is not equilibrated
(rate : less than 50%)

- Upper energy limit formula (Iwata-Otsuka-Maruhn-Itagaki)

Nucleons with the fermi velocity are decisive to the (all the) equilibration :

- rapid process (0.3c)
- independent of relative velocity of collision
- dependence of the sort of colliding nuclei

Calculations and Experiments are well explained.

$$\frac{E_{CE,lab}}{A} = \frac{\hbar^2(3\pi^2\rho_{min})^{2/3}}{2m} + \frac{e^2Z_1Z_2}{4\pi\epsilon_0r_0} \frac{A_1 + A_2}{A_1A_2(A_1^{1/3} + A_2^{1/3})}, \quad (1)$$

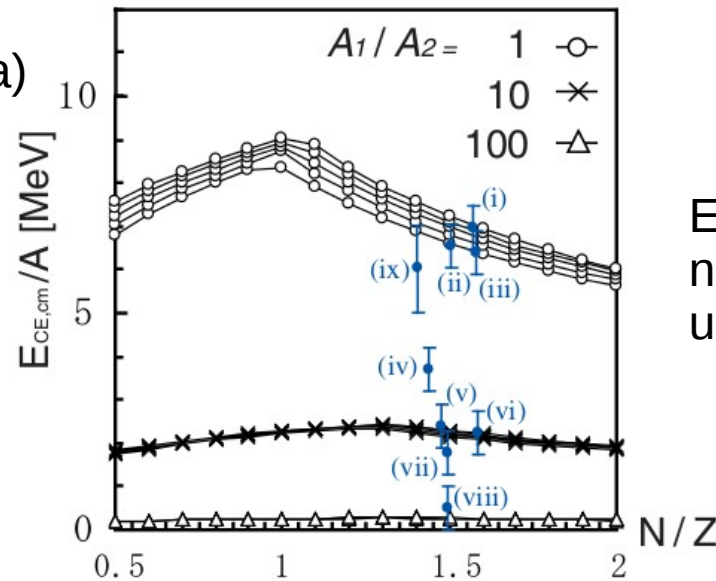
$$\rho_{min} = \min_i \left(\frac{N_i \left(\frac{4\pi r_0}{3} A_i^{1/3} \right)^{-1}}{(1 - 3\bar{\epsilon})(1 + \bar{\delta})}, \frac{Z_i \left(\frac{4\pi r_0}{3} A_i^{1/3} \right)^{-1}}{(1 - 3\bar{\epsilon})(1 - \bar{\delta})} \right), \quad (2)$$

where m , e , ϵ_0 , and r_0 are the nucleon mass, the charge unit, the vacuum permittivity, and the usual nuclear radius parameter (1.2 fm), respectively.

TABLE I. $E_{CE,cm}/A$ values [MeV] obtained by TDHF calculations compared to those obtained by transforming the results of Eq. (1) into the center-of-mass frame. For reference, the values obtained by the Fermi gas model with the standard parameter are also shown.

	Collision	TDHF (SLy4d)	TDHF (SkM*)	Equation (1)	Fermi gas
(i)	$^{208}\text{Pb} + ^{238}\text{U}$	6.5 ± 0.5	6.5 ± 0.5	6.91	9.46
(ii)	$^{208}\text{Pb} + ^{132}\text{Xe}$	6.5 ± 0.5	6.5 ± 0.5	6.50	9.03
(iii)	$^{208}\text{Pb} + ^{132}\text{Sn}$	6.5 ± 0.5	6.5 ± 0.5	6.36	9.03
(iv)	$^{208}\text{Pb} + ^{40}\text{Ca}$	3.5 ± 0.5	3.5 ± 0.5	3.66	5.14
(v)	$^{208}\text{Pb} + ^{24}\text{Mg}$	2.5 ± 0.5	2.5 ± 0.5	2.36	3.52
(vi)	$^{208}\text{Pb} + ^{24}\text{O}$	2.5 ± 0.5	2.5 ± 0.5	2.18	3.52
(vii)	$^{208}\text{Pb} + ^{16}\text{O}$	1.5 ± 0.5	1.5 ± 0.5	1.75	2.50
(viii)	$^{208}\text{Pb} + ^4\text{He}$	<1.0	<1.0	0.48	0.70
(ix)	$^{24}\text{Mg} + ^{24}\text{O}$	5.5 ± 1.0	5.5 ± 1.0	5.99	9.50

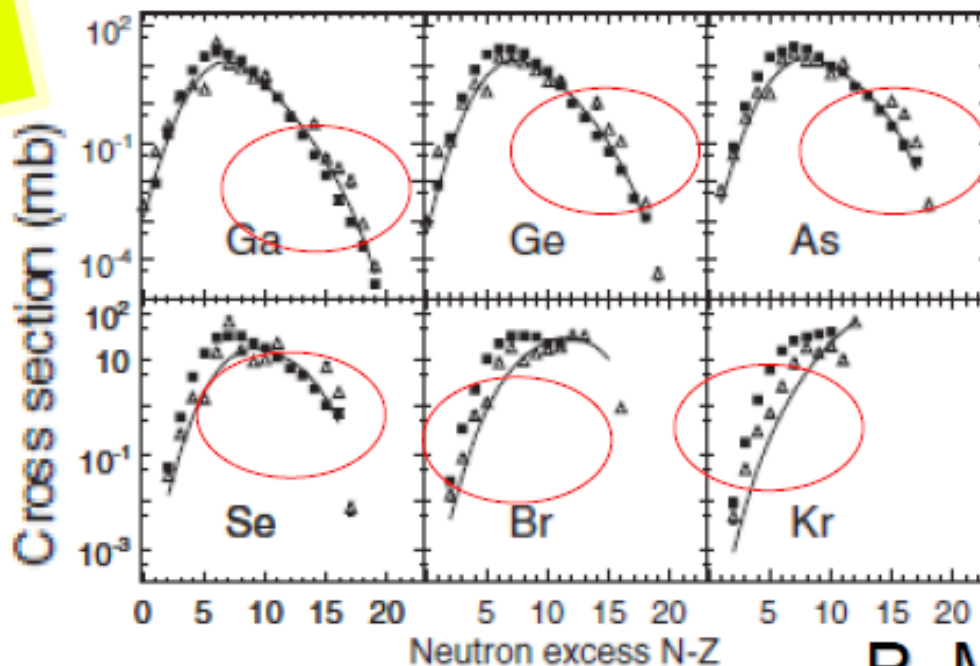
- Dependence of the colliding nuclei (shown by the formula)



Even when the compound nucleus the same, the upper limit can be different.

Experiments

Agree with experiments.



$^{86}\text{Kr} + ^9\text{Be}$

64MeV/A (filled square) v.s. 500MeV/A (open triangle)

Higher yields of exotic elements at higher energies

Other experiments in agreement:

B. Gatty et. al. Nucl. Phys. (1975)

H. Breuer et. al. PRL (1979)

W. P. Tan et. al. PRC (2001)

P. M. Milazzo et. al. PRC (2002)

P. M. Mocko et. al. PRC (2007)

Charge equilibration

- an important mechanism in low-energy heavy-ion collisions -

(Fast) charge equilibration

_ prevents to produce exotic nuclei

decisive mechanism of exotic nuclear synthesis

_ very fast mechanism taking only $\sim 10^{-22}$ s

governing the early stage of heavy-ion collision

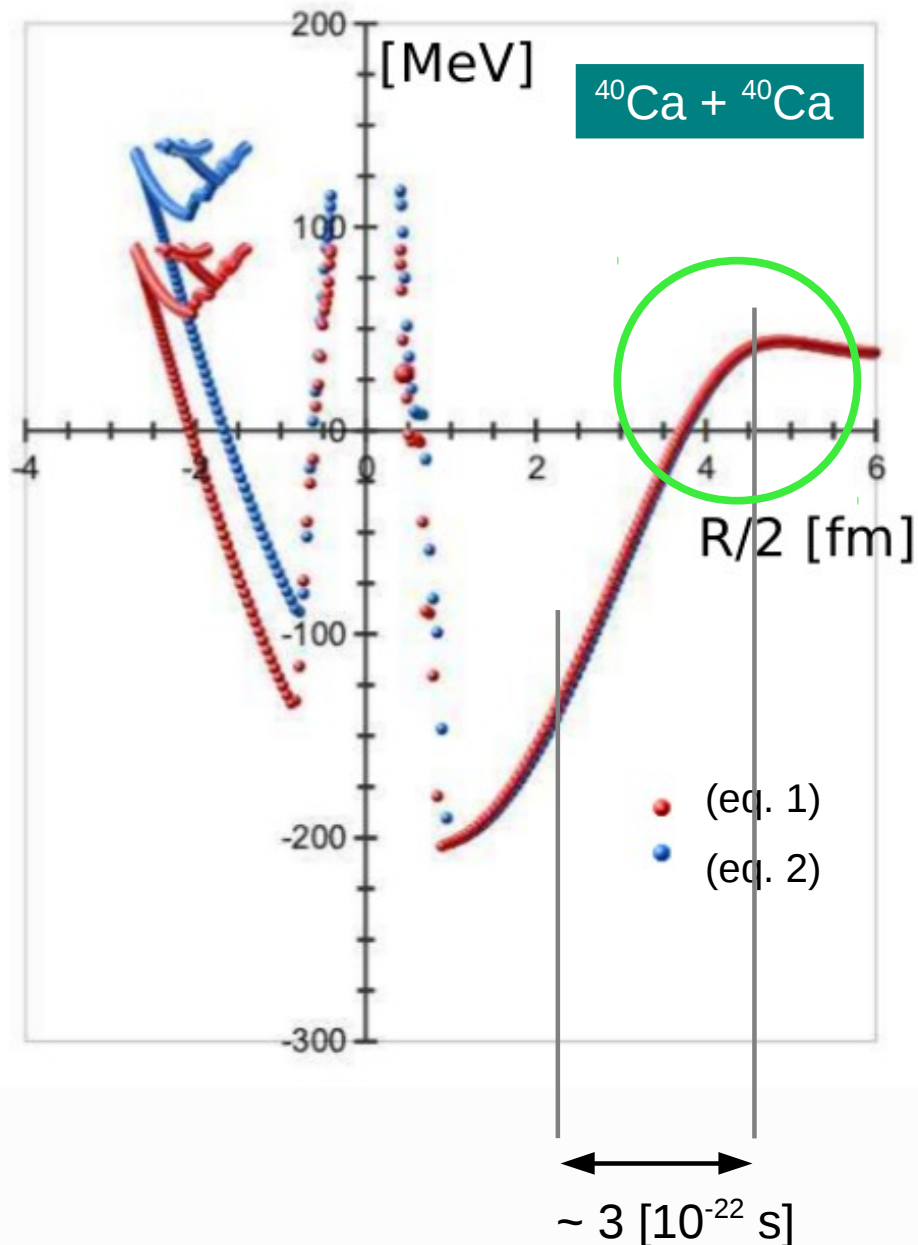
Let us examine this mechanism

with respect to the potential structure

Calculation status for potential

- 3D calculations with 0.8 fm grid-spacing.
- Skyrme:SLy4d and SkM* sets are employed.
- Initial distance is taken to be 20 fm
- $^{16}\text{O}+^{16}\text{O}$, $^{40}\text{Ca}+^{40}\text{Ca}$, $^{56}\text{Ni}+^{56}\text{Ni}$ are calculated;
three different energies

• Charge equilibration in potential



✓ As is well recognized, charge equilibration is a rapid process taking roughly 10^{-22} s, so that it corresponds to $1 < R/2$ [fm] < 4.5 .

✓ For $1 < R/2$ [fm] < 4.5 , the values obtained by (eq. 1) and (eq. 2) are the same; it means there is **no viscosity/friction** in the collective motion of this stage.

✓ As a result, we conclude that charge equilibration is a process without any viscosity. This fact is quite reasonably understood because the charge equilibration is a rapid process dominating the early stage of (low-energy) heavy-ion collisions.

✓ In addition, the effect of window (marked by a green circle) is not the dissipation effect.

Dissipation

- **Wall-window type mechanism**

Dossing-Randrup NPA (1987)

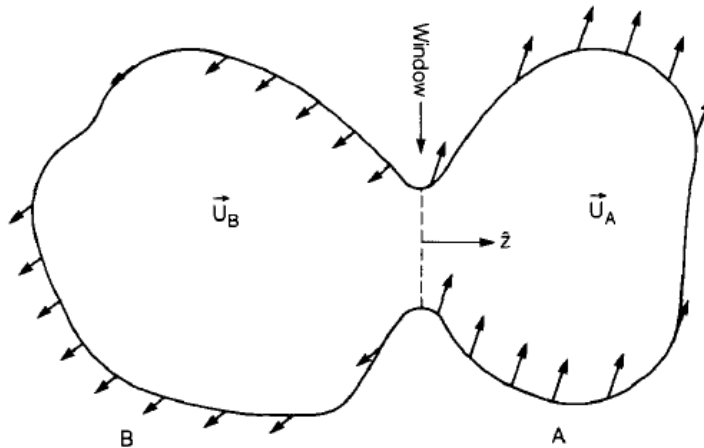


Fig. 1. The dinuclear cavity. In the dinucleus, the individual nucleons move in a leptodermous potential that has two distinct parts, *A* and *B*. The two parts are joined by a small planar “window” whose normal is chosen as the *z*-axis. The two dinuclear parts are endowed with the uniform translational velocities U_A and U_B .

original concept of
dissipation due to the
mean-field

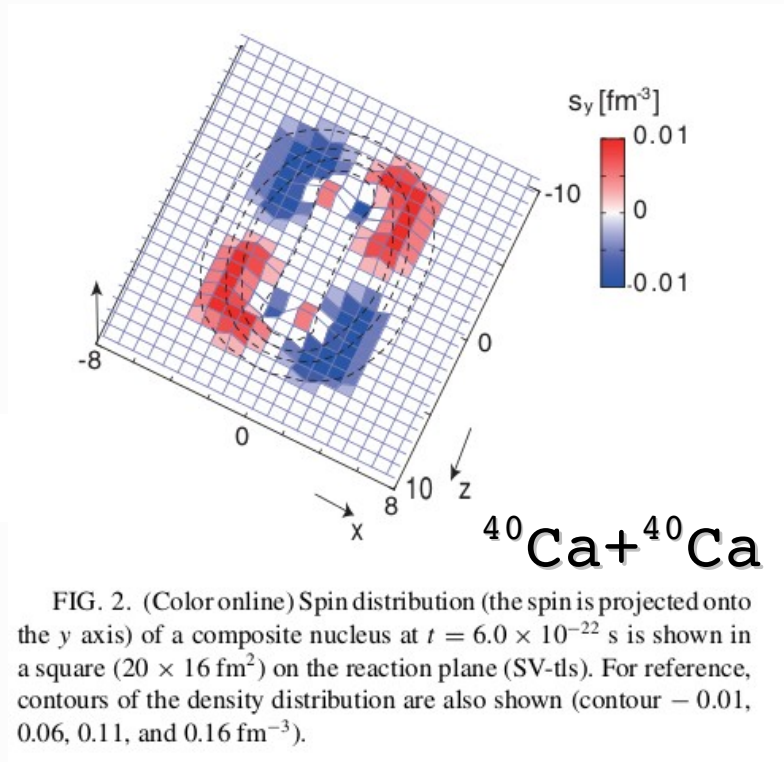
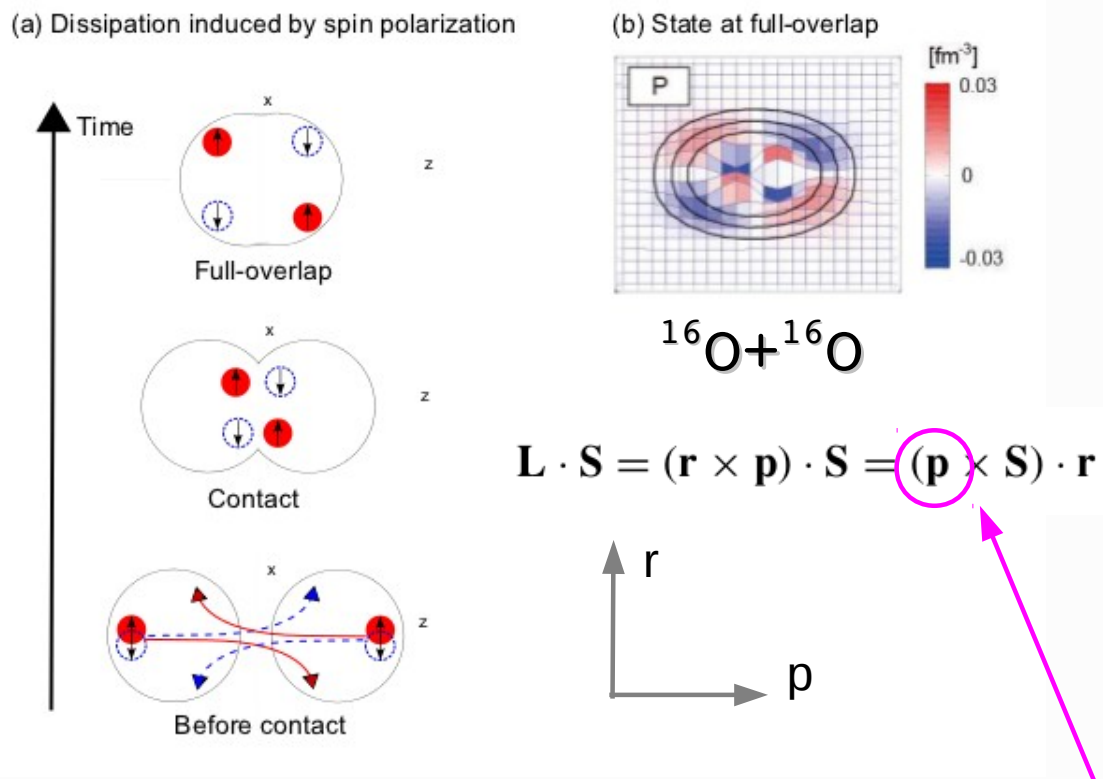
W. J. Swiatecki, *Phys. Scripta* **24** 113 (1981); J. Randrup and W. J. Swiatecki, *Nucl. Phys.* **A429** 105 (1984).

- **Other mechanism**

Spin-orbit force (for the fusion-window problem)

Tensor force (dynamically interesting; Y.I.-Maruhn, *PRC* (2011))

- Dissipation due to the spin-orbit force, which is actually calculated in spatial 3D framework



Y.I., to appear IJMPE

Y.I.-Maruhn, PRC (2011)

- Spin-orbit effect is necessary to decelerate colliding nuclei after the touching
- This dissipation holds very strong momentum-dependence
- Spin-orbit effect is highly related to the axial symmetry breaking of the dynamics

- Dissipation due to the Spin-Orbit force

The collision, which does not result in fusion in the previous TDHF calculations

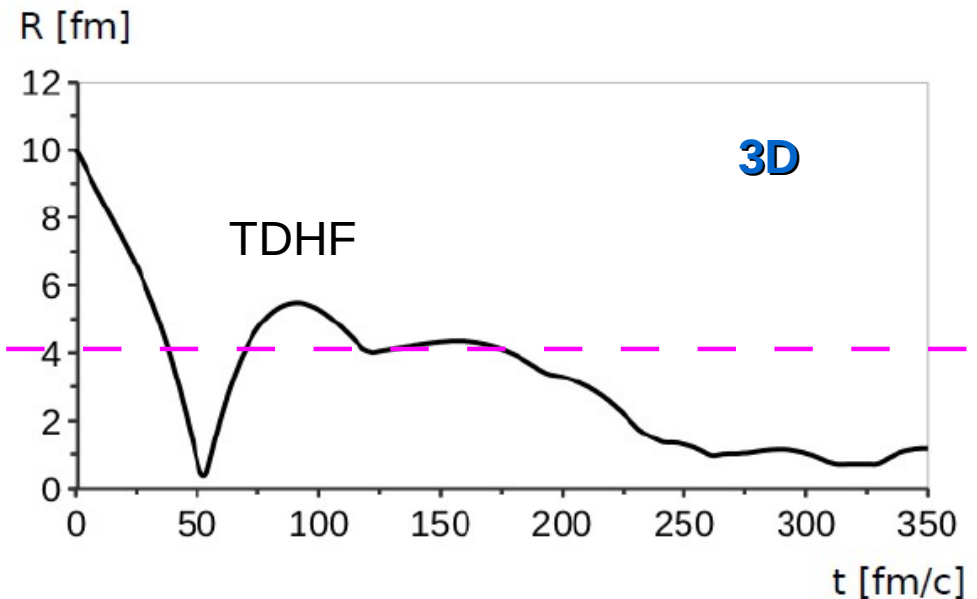
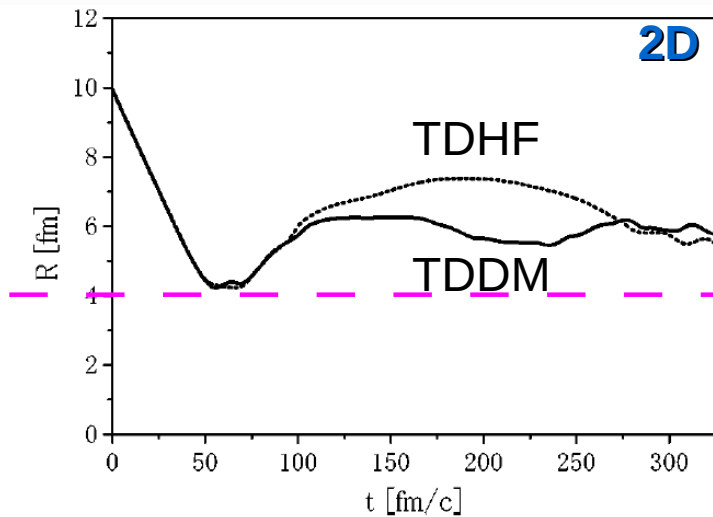


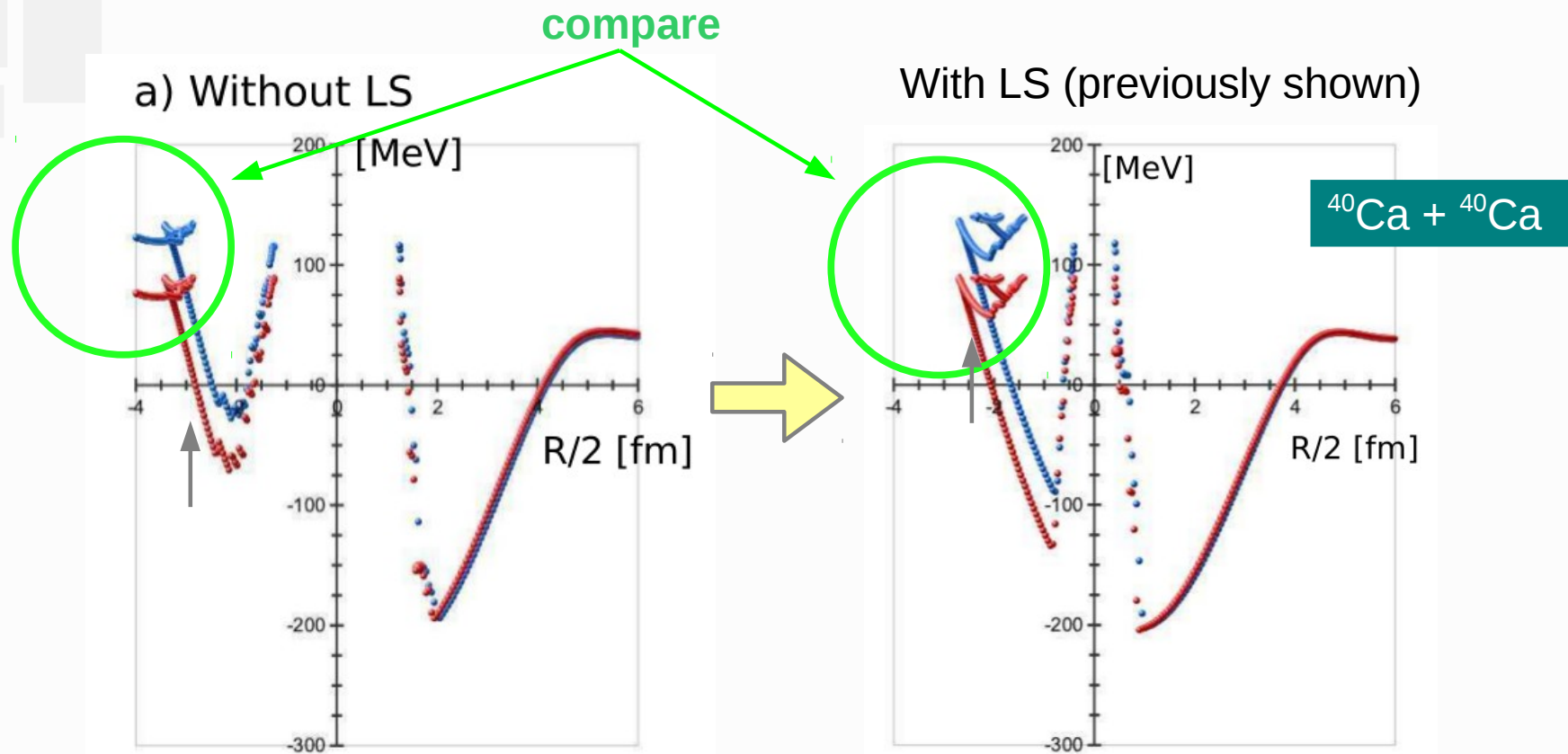
FIG. 1. Time evolution of the relative distance in a head-on collision of $^{16}\text{O} + ^{16}\text{O}$ at $E_{\text{c.m.}} = 65$ MeV calculated in TDHF (dotted line) and TDDM (solid line).

Tohyama-Umar PRC (2001)

Fig.1 of “Y.I., to appear in EPJW (CNR*11)”

- The increase of dissipation due to the spin-orbit force is noticed
it contributes to eliminate non-physical fusion window
- The effect of spatial dimension is larger than the higher-order contribution !

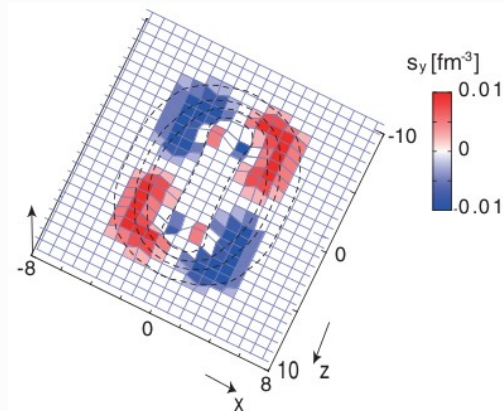
• Dynamic spin-orbit force effect in the potential



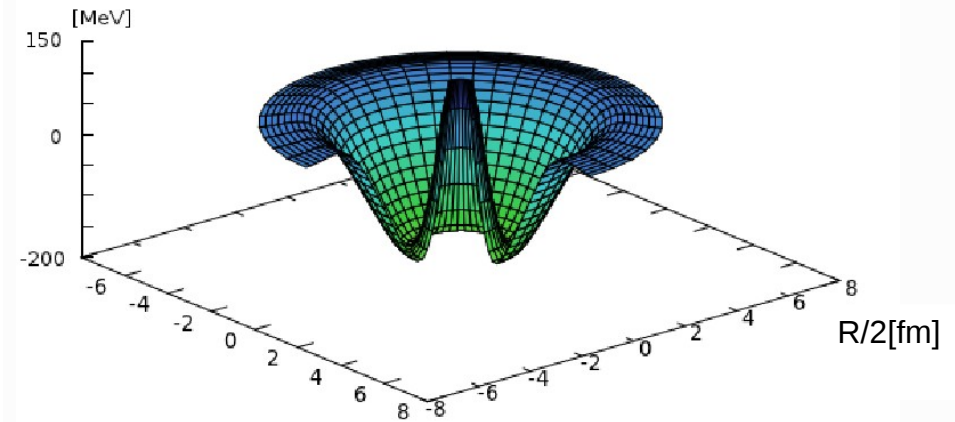
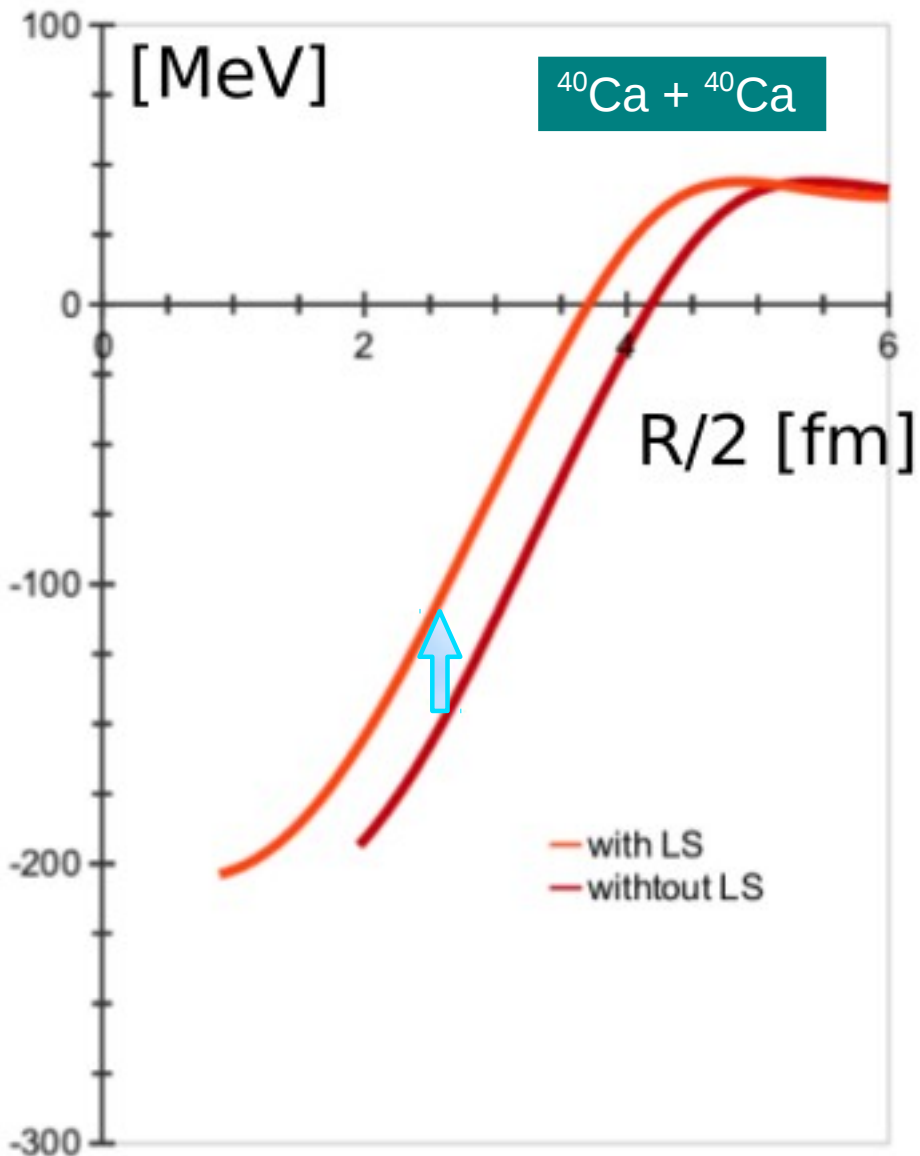
✓ LS force is decisive to whether fusion appears or not (see **Green circles**).

✓ Large difference can be found in the short-range repulsive core ($|R| < 1$ fm), while only small difference is seen in the entrance stage ($R > 3$).
 → in particular, the width of short range core is changed.

✓ The amount of stopping energy due to LS force is roughly 50 MeV (see Gray arrow).



b) LS effect



[3D View] Nucleus-nucleus potential for $^{40}\text{Ca} + ^{40}\text{Ca}$

- ✓ The shape/width of nucleus-nucleus potential is changed by LS force.
 - if LS force is present, the range of repulsive core shrinks.
- ✓ To a lesser degree, the fusion barrier is changed; a bit lower height at larger R .
- ✓ At fixed R , deceleration effect (the reduction of attractive force) arises from the LS force. It is roughly 40 MeV for $2 < R/2$ [fm] < 4 .

Multi-dimensional potential plot will be available after introducing finite Impact parameter

- Dissipation due to the spin-orbit force

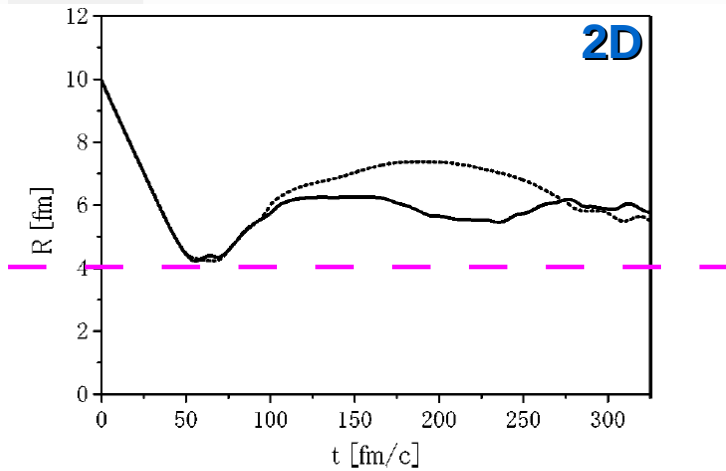


FIG. 1. Time evolution of the relative distance in a head-on collision of $^{16}\text{O}+^{16}\text{O}$ at $E_{c.m.}=65$ MeV calculated in TDHF (dotted line) and TDDM (solid line).
Tohyama-Umar PRC (2001)

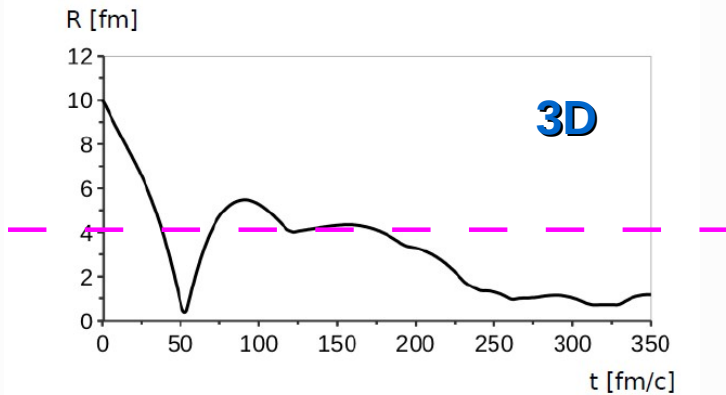


Fig.1 of “Y.I., to appear in EPJW (CNR*11)”

Nucleus-nucleus potential from TD-DFT

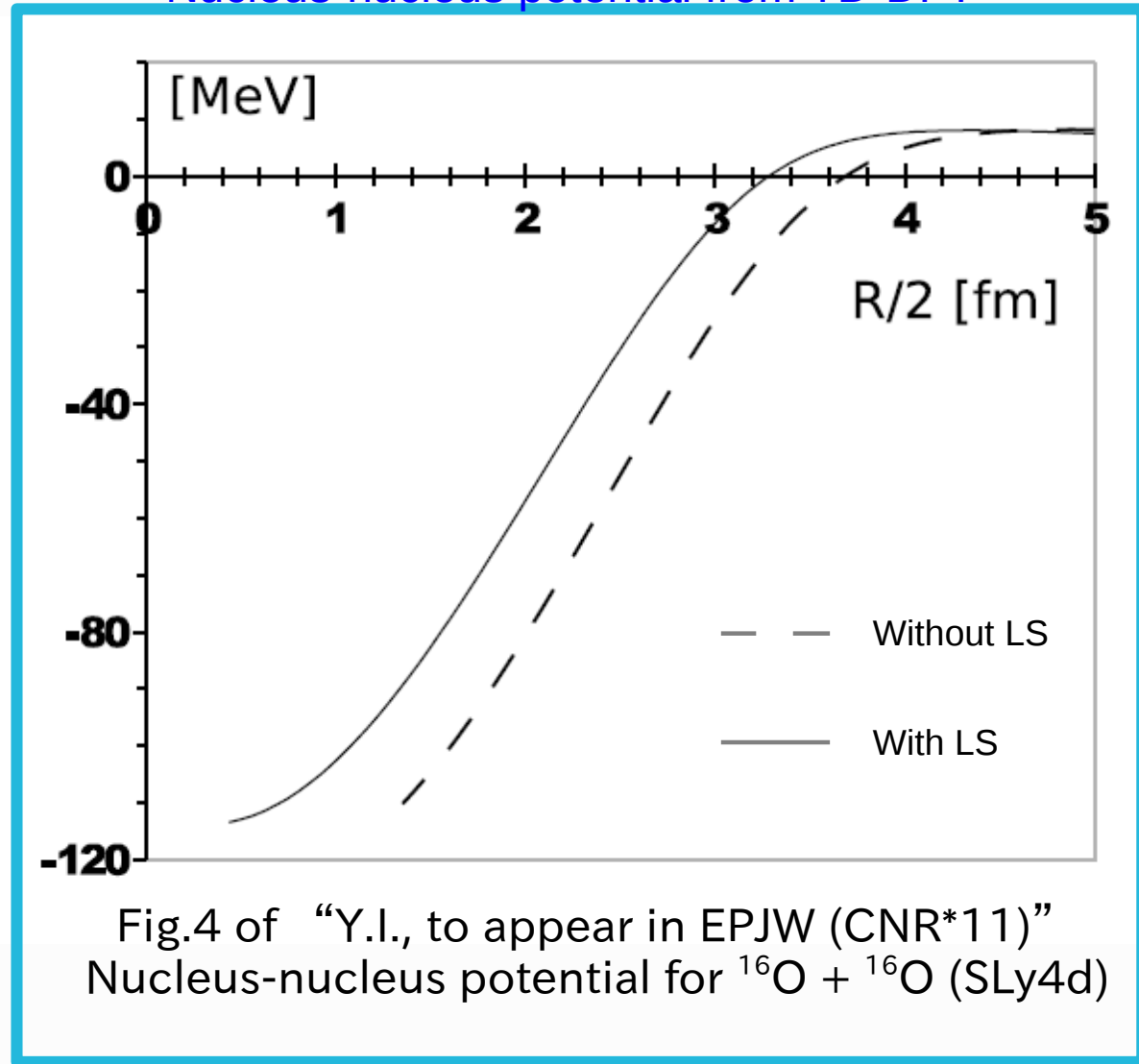


Fig.4 of “Y.I., to appear in EPJW (CNR*11)”
Nucleus-nucleus potential for $^{16}\text{O} + ^{16}\text{O}$ (SLy4d)

- The increase of dissipation due to the spin-orbit force is nothing to do with the wall and the window.
- Alternatively, its dependence on the spatial-dimension and the momentum is remarkable.

- Dissipation due to the tensor force

$$\mathbf{W}_q(\mathbf{r}) \cdot (-i)(\nabla \times \boldsymbol{\sigma}),$$

$$\mathbf{W}_q(\mathbf{r}) = \mathbf{W}_q^{LS}(\mathbf{r}) + \mathbf{W}_q^T(\mathbf{r}),$$

As a modification of spin-orbit force

- Tensor force effect becomes 5 to 10 times larger in collision situations
- As is shown in the form factor, the tensor effect modifies the spin-orbit effect
- Tensor effect compared to spin-orbit effect becomes larger for heavier nuclei

Form factor of the spin mean-field

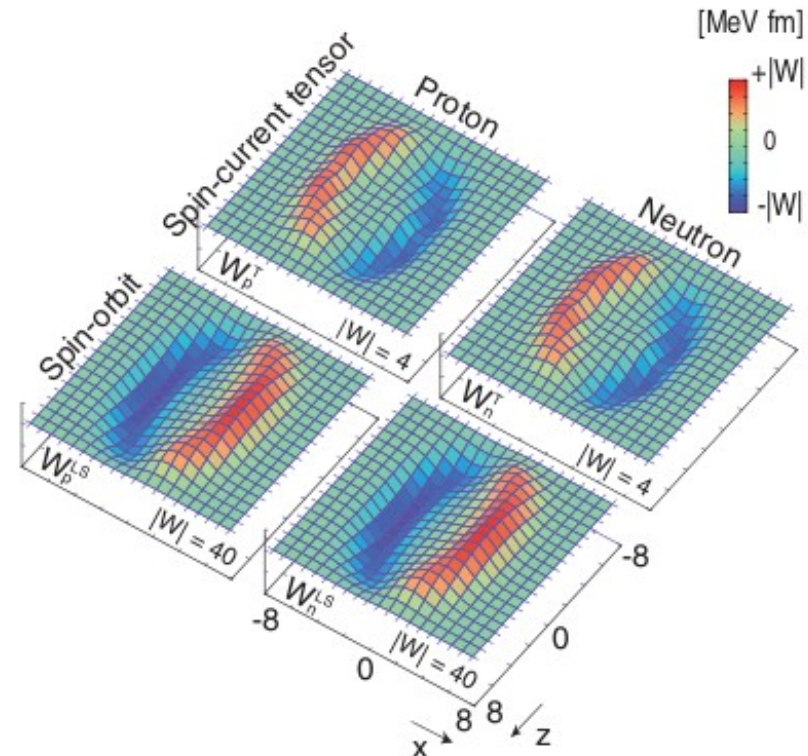


FIG. 3. (Color online) Snapshots of the x component of $\mathbf{W}_q(\mathbf{r})$ at $t = 6.0 \times 10^{-22}$ s projected on the reaction plane (SV-tilt). The values are plotted in a square ($16 \times 16 \text{ fm}^2$) on the reaction plane separately for the spin-current tensor and spin-orbit contributions, and for protons ($q = p$) and neutrons ($q = n$), respectively. The maximum amplitude $|W|$ of the function is shown in the lower right-hand side of each plot.

New dissipation mechanism different from wall-window type

- Spin-orbit and tensor forces cause the dissipation
- This type of dissipation is directly connected with the spin polarization, where the dynamics perpendicular to the reaction axis is important.
- Accordingly, it is different from the existence of wall and the width of window (even within the mean-field type dissipation)
- This type of dissipation is momentum dependent. It is quite difficult to explain momentum dependence merely by the wall-window type mechanism

Summary

- We have established our own method of extracting nucleus-nucleus potential from diabatic time evolution (heavy-ion collision; far from the thermal equilibrium).
- Some important reaction mechanisms are explained in terms of the potential.
 - _ Charge equilibrium is identified to be the effect without viscosity
 - _ Dynamical LS-force effect is visualized in the context of potential (for the first time) as well as the tensor force effect.
 - _ Importance of dissipation nothing to do with wall-window mechanism

Remark for Washiyama-Lacroix PRC (2008) & Washiyama-Lacroix-Ayik PRC (2009)

- The dissipation in 3d-TDHF was shown for the first time.
- The obtained potential is concluded to be equal to the Umar's adiabatic potential.
 - it is difficult to understand. Is the statement of such a coincidence itself physical ???
- Large dissipation 30MeV in $O^{16}+O^{16}$ in the entrance channel (total E = several 10 MeV), and corresponds to the adiabatically calculated dissipation
 - it is difficult to believe. Is the optical potential calculated in TDHF ???
- We afraid that there might be a systematic error in the Washiyama-san's method on deriving potential